FOREX Publication
Open Access | Rapid and quality publishing

International Journal of
Electrical and Electronics Research (IJEER)
Research Article | Volume 11, Issue 4 | Pages 1022-1029 | e-ISSN: 2347-470X

Performance Analysis of Sensorless Induction Motor Drive using Improved Control Techniques

Santosh Yadav[1] and Dr. N. R. Bhasme[2]
[1]*Research Scholar, Department of Electrical Engineering, Government College of Engineering, Aurangabad, India, princesantoshyadav@gmail.com*
[2]*Associate Professor, Department of Electrical Engineering, Government College of Engineering, Yavatmal, India, nrbhasme@yahoo.com*

***Correspondence:** *Santosh Yadav; princesantoshyadav@gmail.com*

ABSTRACT- AC Drives demand robust motor design with rugged construction, low cost, high reliability in service, and simple maintenance. In modern power drives, Sensorless Induction motor drives are more popular than other drives. A speed sensor/encoder-based drive is costlier and requires more space in case more parallel units are coupled together in drive operation. To address these difficulties, speed Sensorless drives are introduced without loss of efficiency and reliability. However, Sensorless speed drive requires advanced control techniques in which complex calculations are there due to the nonlinearity of IM. In the recent past, Machine model-based methods *i.e.*, MRAS (Model reference adaptive systems) and ELO (Extended Luenberger observer) have been popularized due to ease of implementation compared to other techniques. In this work, improved MRAS and ELO models are implemented and verified using Simulink software. Then, the same is validated with the help of an FPGA (field programmable gate array) based Snetly real-time controller. The key improvements are achieved as follows: effective speed estimation, robust speed tracking, reduced speed estimation error, and robust stability which helps to enhance the transient and steady-state performance of the drive.

Keywords: ELO, IFOC, Induction Motor, MRAS, Sensorless, Snetly controller.

ARTICLE INFORMATION
Author(s): Santosh Yadav and Dr. N.R. Bhasme;
Received: 16/09/2023; **Accepted**: 30/10/2023; **Published**: 20/11/2023;
e-ISSN: 2347-470X;
Paper Id: IJEER 1609-11;
Citation: 10.37391/IJEER.110420
Webpage-link:
https://ijeer.forexjournal.co.in/archive/volume-11/ijeer-110420.html

Publisher's Note: FOREX Publication stays neutral with regard to Jurisdictional claims in Published maps and institutional affiliations.

1. INTRODUCTION

Induction Motor (IM) is served widely in many industries due to simple structure, sturdy construction, excellent dependability, low cost, and low maintenance [1]. A speed encoder is placed on the rotor shaft to get rotor speed. In this case, additional space is required to accommodate it between the motor and the controller. In closed loop drives, a speed sensor causes certain problems like reduction of electro-mechanical structure of the drive, reliability issues in hostile and hazardous environments, shaft extension required, and increased cost [2]. To address this, a speed Sensorless drive operation is preferred over speed encoder-based drives [3]. However, there are a few other gaps that need to be improved in the case of speed Sensorless drives [4]. These drives are suffered from loss of stability and reliability at zero and very low frequencies [5]. There are numerous advanced control techniques have been suggested for IM in different topologies in the recent past [6]. Indirect Field oriented control (IFOC) Vector-control drives are preferred over scalar-controlled drives due to higher accuracy and better stability [7]. Later, speed Sensorless vector-controlled IM drives are very popular for higher-performance applications [8], [9]. Among various techniques, model-based speed estimation techniques are providing flexibility to implement easily with higher dynamic performance. Each of the methods has its merit and demerits. These techniques are named; Model reference adaptive system (MRAS), Sliding mode observer (SMO), and other Artificial Intelligence (AI) techniques, Extended Kalman filter (EKF), Extended Luenberger observer (ELO) [8], [10]–[14].

In the recent past, many improved methods have been suggested to counter the issues at low frequencies [15]. The problems associated with stability and poor speed estimations have led the research to progress in this area [16]. There is a need to implement advanced real prototyping digital controllers to fetch accurate information from the rotor and machine parameters [17]. Some of the above methods are more sensitive to machine parameters which cause errors in flux and speed estimation. The main objectives of drives are to achieve robust speed tracking, minimize speed error (actual vs reference), have higher stability, and be less sensitive to machine and other dependent parameters. A few applications like Electric vehicle (EVs) demands accurate speed estimation and robust stable operation in lower, medium, and higher speed ranges within short periods [18]. However, the implementation of advanced control algorithms requires more space and memory. Generally, non-linear machines are of having complex equations and implementation is difficult in motor controller-based electric drives [19]. The continuous progress and developments have been thoroughly done due to modern evaluation in power electronics and embedded industry [20]. In such cases, these

FOREX Publication
Open Access | Rapid and quality publishing
International Journal of Electrical and Electronics Research (IJEER)
Research Article | Volume 11, Issue 4 | Pages 1022-1029 | e-ISSN: 2347-470X

modern real prototyping controllers are highly preferred to implement complex algorithms of modern drives [21]. Modern controllers are required to implement complex algorithms [10], [22]–[26]. These algorithms required more computations, memory, and processing speed [27]. In the power and industrial sector, continuous drive monitoring is required to understand the drive performance. FPGA is a powerful tool for heavy control algorithms due to its advantages in logic resources and multiple I/O pins [28]. Improving the control performance by fully utilizing the switching frequency is the key parameter. Digital controllers are required high-fidelity modeling, high control bandwidth, and low latency [29]. In this work, improved MRAS and ELO control algorithms are presented to analyze the drive performance. The drive is implemented with MRAS, ELO algorithms in MATLAB/Simulink software. A new Snetly rapid prototyping real time controller is used to capture more data with less computation time. The Simulink results are shown improved dynamic performance and a robust, good speed tracking profile under different loading conditions. Also, improved speed estimation and minimum speed error have been found with these improved algorithms.

The system design is modelled with equations are described in section 2 and in subsections, MRAS and ELO algorithms, and their implementation is presented using Snetly controller. The performance analysis and concern results are discussed in detail in *section 3*. Then, Conclusion is presented in *section 4*.

2. METHODS AND MODEL

2.1 Dynamic Modelling of IM

IM model dynamic model with the synchronous speed in the d-q reference frame can be written as [30]:

$$\frac{dI_{sd}}{dt} = -\lambda I_{sd} + \omega_s I_{sq} + \frac{k_s}{T_s}\varphi_{rd} + \omega k_s \varphi_{rq} + \frac{1}{\sigma L_s} V_{sd} \quad (1)$$

$$\frac{dI_{sq}}{dt} = -\omega_s I_{sd} - \lambda I_{sq} + \frac{k_s}{T_s}\varphi_{rq} - \omega k_s \varphi_{rd} + \frac{1}{\sigma L_s} V_q \quad (2)$$

$$\frac{d\varphi_{rd}}{dt} = \frac{M}{T_r} I_{sd} - \frac{1}{T_r}\varphi_{rd} + (\omega_s - \omega)\varphi_{rq} \quad (3)$$

$$\frac{d\varphi_{rq}}{dt} = \frac{M}{T_r} I_{sq} - (\omega_s - \omega)\varphi_{rd} - \frac{1}{T_r}\varphi_{rq} \quad (4)$$

Torque and mechanical expressions are to be written as

$$C_e = p\frac{M}{L_r}(\varphi_{rd} I_{sq} - \varphi_{rq} I_{sd}) \quad (5)$$

$$\frac{d\Omega}{dt} = (C_e - C_r - f_r\Omega)/J \quad (6)$$

$$\sigma = 1 - \frac{M^2}{L_s L_r}; k_s = \frac{M}{\sigma L_s L_r} = \frac{1-\sigma}{M\sigma}; \lambda = \frac{1}{T_s\sigma} + \frac{1-\sigma}{T_r\sigma} \quad (7)$$

2.2 IFOC Algorithm

According to the IFOC principle, the decoupling of flux and torque could cause an IM to behave similarly to a DC Motor. In this situation, the next need must be met. The rotor flux direction and the rotating frame's d-axis orientation are in alignment.

$$\varphi_{rd} = \varphi_r, \varphi_{rq} = 0 \quad (8)$$

Equation (1) & *(2)* can be re-written as

$$\begin{cases} V_{sd} = V_{sd}^{'} - E_d \\ V_{sq} = V_{sq}^{'} - E_q \end{cases} \quad (9)$$

The new decoupled equation becomes,

$$\begin{cases} V_{sd}^{'} = \sigma L_s \frac{dI_{sd}}{dt} + \lambda\sigma L_s I_{sd} \\ V_{sq}^{'} = \sigma L_s \frac{dI_{sq}}{dt} + \lambda\sigma L_s I_{sq} \end{cases} \quad (10)$$

The torque equation becomes,

$$C_e = p\frac{M}{L_r}(\varphi_{rd} I_{sq}) \quad (11)$$

Equation (3) & *(4)* becomes

$$\begin{cases} \varphi_r = M I_{sd} \\ (\omega_s - \omega) = \frac{M I_{sq}}{T_r \varphi_r} \end{cases} \quad (12)$$

The d-q reference frame is moving with,

$$\theta_s = \int \frac{I_{sq}}{T_r I_{sd}} + \theta \quad (13)$$

Snetly controller work flow and hardware setup are as shown in *figure 1* and *figure 2* respectively. Also, symbols and their terms have been presented in *section 3*.

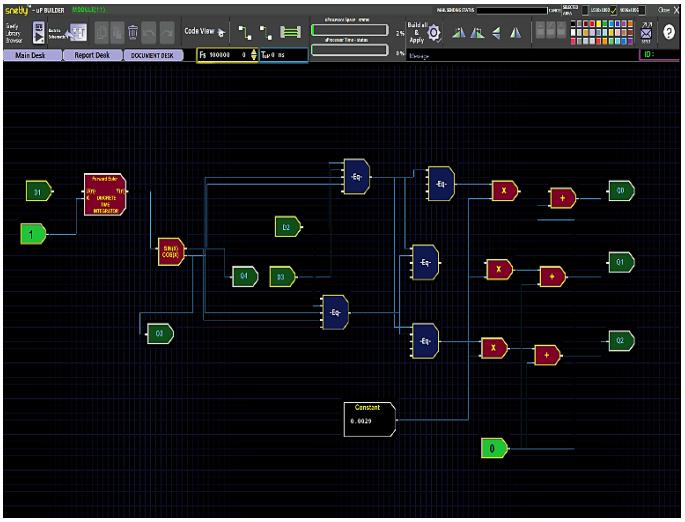

Figure 1: Snetly real-time controller workflow

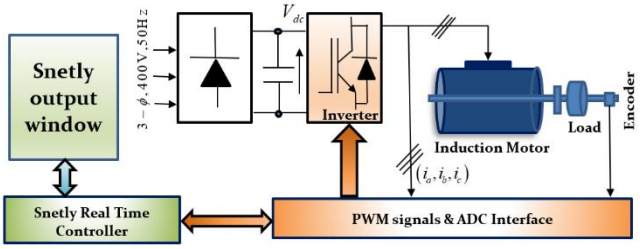

Figure 2: Snetly based IM drive [27]

FOREX Publication
Open Access | Rapid and quality publishing
International Journal of Electrical and Electronics Research (IJEER)
Research Article | Volume 11, Issue 4 | Pages 1022-1029 | e-ISSN: 2347-470X

2.3 MRAS based Sensorless IFOC IM drive

The Reference and Adjustable models are the two models available to the MRAS observer. The reference model and the adjustable model are related to the voltage model and the current model, respectively. Using Stationary $\alpha-\beta$ reference frame of IM model, the following equations are derived.

$$\begin{cases}\frac{d(\varphi_{r\alpha})_{ref}}{dt}=\frac{Lr}{M}\left(V_{s\alpha}-R_sI_{s\alpha}-\sigma L_s\frac{dI_{s\alpha}}{dt}\right)\\ \frac{d(\varphi_{r\beta})_{ref}}{dt}=\frac{Lr}{M}\left(V_{s\beta}-R_sI_{s\beta}-\sigma L_s\frac{dI_{s\beta}}{dt}\right)\end{cases} \quad (14)$$

$$\begin{cases}\frac{d(\varphi_{r\alpha})_{ad}}{dt}=-\beta(\varphi_{r\alpha})_{ad}-\omega\left(\varphi_{r\beta}\right)_{ad}+M\beta I_{s\alpha}\\ \frac{d(\varphi_{r\beta})_{ad}}{dt}=-\beta\left(\varphi_{r\beta}\right)_{ad}+\omega(\varphi_{r\alpha})_{ad}+M\beta I_{s\beta}\end{cases} \quad (15)$$

The estimation error vector derivative can become,

$$\dot{e}_{\alpha\beta}=X_{MRAS}e_{\alpha\beta}-Y_{MRAS} \quad (16)$$

here,

$$X_{MRAS}=\begin{bmatrix}-\beta & -\omega & 0 & 0\\ \omega & -\beta & 0 & 0\\ 0 & 0 & 0 & 0\\ 0 & 0 & 0 & 0\end{bmatrix}$$

Using Lyapunov function,

$$V=e_{\alpha\beta}^Te_{\alpha\beta}+\frac{(\omega-\hat{\omega})^2}{\delta_\omega}+\frac{(R_s-\hat{R}_s)^2}{\delta_{R_S}}+\frac{(\beta-\hat{\beta})^2}{\delta_\beta} \quad (17)$$

The time derivative of V become,

$$\dot{V}=\frac{de_{\alpha\beta}^T}{dx}e_{\alpha\beta}+e_{\alpha\beta}^T\frac{de_{\alpha\beta}}{dx}-\frac{2}{\delta_\omega}\Delta\omega\frac{de_{\alpha\beta}}{dt}-\frac{2}{\delta_{R_S}}\Delta R_s\frac{d(\hat{R}_s)}{dt}-\frac{2}{\delta_\beta}\frac{d(\hat{\beta})}{dt} \quad (18)$$

$$Y_{MRAS}=\begin{bmatrix}\Delta\beta & \Delta\omega & -M\Delta\beta & 0\\ -\Delta\omega & \Delta\beta & 0 & -M\Delta\beta\\ 0 & 0 & -\frac{Lr}{M}\Delta R_s & 0\\ 0 & 0 & 0 & \frac{Lr}{M}\Delta R_s\end{bmatrix}\begin{bmatrix}(\hat{\varphi}_{r\alpha})_{ad}\\ \left(\hat{\varphi}_{r\beta}\right)_{ad}\\ I_{s\alpha}\\ I_{s\beta}\end{bmatrix}$$

$$\Delta\omega=\omega-\hat{\omega},\Delta R_s=R_s-\hat{R}_s,\Delta\beta=\beta-\hat{\beta}$$

The speed estimation term would be,

$$\hat{\omega}=\int\delta_\omega\left[(\hat{\varphi}_{r\alpha})_{ad}\left(\hat{\varphi}_{r\beta}\right)_{ref}-\left(\hat{\varphi}_{r\beta}\right)_{ad}(\hat{\varphi}_{r\alpha})_{ref}\right] \quad (19)$$

To modify pure integration in the above equation, the below Improved algorithm has been proposed.

Let,

$$m=\int\delta_\omega\left[(\hat{\varphi}_{r\alpha})_{ad}\left(\hat{\varphi}_{r\beta}\right)_{ref}-\left(\hat{\varphi}_{r\beta}\right)_{ad}(\hat{\varphi}_{r\alpha})_{ref}\right] \quad (20)$$

Correction Factor, $\lambda_1=(\omega-m)$ (21)

$$H=\begin{cases}\lambda_1 \;;\; if\ \omega\neq m\\ 0 \;\;;\; if\ \omega\leq m\end{cases} \quad (22)$$

Hence, Estimation Speed can be $\hat{\omega}=m+H$ (23)

This Correction factor is helpful when estimation error is produced. In case of zero and very low frequencies, Improved MRAS provides a good solution to overcome poor stability and accuracy in speed estimation applications.

2.4 ELO based Sensorless IM drive

The motor model can be written with respect to state equations in the $\boldsymbol{\alpha-\beta}$ reference frame.

$$\begin{cases}\dot{\hat{X}}=A.X+B.U\\ Y=C.X\end{cases} \quad (24)$$

here,

$$X=[i_{s\alpha}i_{s\beta}\ \phi_{r\alpha}\ \phi_{r\alpha}\ \phi_{r\beta}]^T$$
$$U=[v_{s\alpha}v_{s\beta}]^T$$
$$Y=[i_{s\alpha}i_{s\beta}]^T$$

The state equations are,

$$\begin{cases}\dot{\hat{\imath}}_{s\alpha}=a_1.i_{s\alpha}+a_2.\phi_{r\alpha}-a_3.\omega_r.\phi_{r\alpha}+a_6.v_{s\alpha}\\ \dot{\hat{\imath}}_{s\beta}=a_1.i_{s\beta}+a_2.\phi_{r\beta}+a_3.\omega_r.\phi_{r\alpha}+a_6.v_{s\beta}\\ \dot{\hat{\phi}}_{r\alpha}=a_4.i_{s\alpha}+a_5.\phi_{r\alpha}-\omega_r.\phi_{r\beta}\\ \dot{\hat{\phi}}_{r\beta}=a_4.i_{s\beta}+a_5.\phi_{r\beta}+\omega_r.\phi_{r\alpha}\end{cases} \quad (25)$$

here,

$$a_1=-\frac{1}{\sigma T_s}-\frac{(1-\sigma)}{\sigma T_r};a_2=\frac{L_m}{\sigma L_sL_r}\frac{1}{T_r};a_3=-\frac{L_m}{\sigma L_sL_r};$$
$$a_4=\frac{L_m}{T_r};a_5=-\frac{1}{T_r};a_6=\frac{1}{\sigma T_s}$$

The gain matrix is,

$$K=\begin{bmatrix}K_1 & -K_2\\ K_2 & K_1\\ K_3 & -K_4\\ K_4 & K_3\end{bmatrix} \quad (26)$$

In this case, speed is unknown parameter. So, the unknown parameter speed can be obtained by identifying the adaptation law.

$$A_{\omega_r}=\begin{bmatrix}a_1 & 0 & a_2 & -a_3\hat{\omega}\\ 0 & a_1 & -a_3\hat{\omega} & a_2\\ a_4 & 0 & a_5 & -\hat{\omega}_r\\ 0 & a_4 & \hat{\omega}_r & a_5\end{bmatrix};$$

$$(I_s-\hat{I}_s)=[I_{s\alpha}\ -\hat{I}_s\ I_{s\beta}\ -\hat{I}_s];$$

Hence, the observer estimated quantity (Speed) can be written as,

$$\dot{\hat{X}}=A_{\omega_r}(\hat{\omega}_r)\hat{X}+BU+K(I_s-\hat{I}_s) \quad (27)$$

Here, the estimation error of rotor flux and stator current can be written as

$$\dot{e}=(A-KC)e+(\Delta A)\hat{X} \quad (28)$$

here,

FOREX Publication
Open Access | Rapid and quality publishing
International Journal of Electrical and Electronics Research (IJEER)
Research Article | Volume 11, Issue 4 | Pages 1022-1029 | e-ISSN: 2347-470X

$$\Delta A = A(\omega_r) - A(\hat{\omega}_r) = \begin{bmatrix} 0 & 0 & 0 & a_3\Delta\omega_r \\ 0 & 0 & -a_3\Delta\omega_r & 0 \\ 0 & 0 & 0 & -\Delta\omega_r \\ 0 & 0 & \Delta\omega_r & 0 \end{bmatrix}$$

$$\Delta\omega_r = \omega_r - \hat{\omega}_r$$

$$e = X - \hat{X} = [e_{I_{s\alpha}} e_{I_{s\beta}}\ e_{\Psi_{s\alpha}} e_{\Psi_{s\beta}}]^T$$

$$\begin{cases} K_1 = (k-1)\left(\frac{1}{\sigma T_s} + \frac{(1-\sigma)}{\sigma T_r} + \frac{1}{T_r}\right) \\ K_2 = (k-1)\hat{\omega}_r \\ K_3 = \frac{(1-k^2)}{a_3}\left(\frac{1}{\sigma L_s} + \frac{(1-\sigma)}{\sigma T_r} + \frac{a_3}{T_r}\right) + \\ \qquad + \frac{(k-1)}{a_3}\left(\frac{1}{\sigma T_s} + \frac{(1-\sigma)}{\sigma T_r} + \frac{1}{T_r}\right) \\ K_4 = \frac{(k-1)}{a_3}\hat{\omega}_r \end{cases}$$

The Lyapunov function can be written as

$$V = e^T e + \frac{(\omega - \hat{\omega}_r)^2}{\lambda} \quad (29)$$

The Lyapunov function derivative becomes

$$\frac{dV}{dt} = \left\{\frac{de^T}{dt}\right\} e + e^T \left\{\frac{de}{dt}\right\} + \frac{d}{dt}\left\{\frac{(\omega - \hat{\omega}_r)^2}{\lambda}\right\} \quad (30)$$

Using PI controller, speed estimation is given by

$$\hat{\omega}_r = K_p(e_{I_{s\alpha}}\hat{\phi}_{r\beta} - e_{I\beta}\hat{\phi}_{r\alpha}) + \frac{K_i}{s}\int(e_{I_{s\alpha}}\hat{\phi}_{r\beta} - e_{I\beta}\hat{\phi}_{r\alpha})dt \quad (31)$$

In this work, effective K_p, K_i gains are tuned to achieve robust speed tracking.

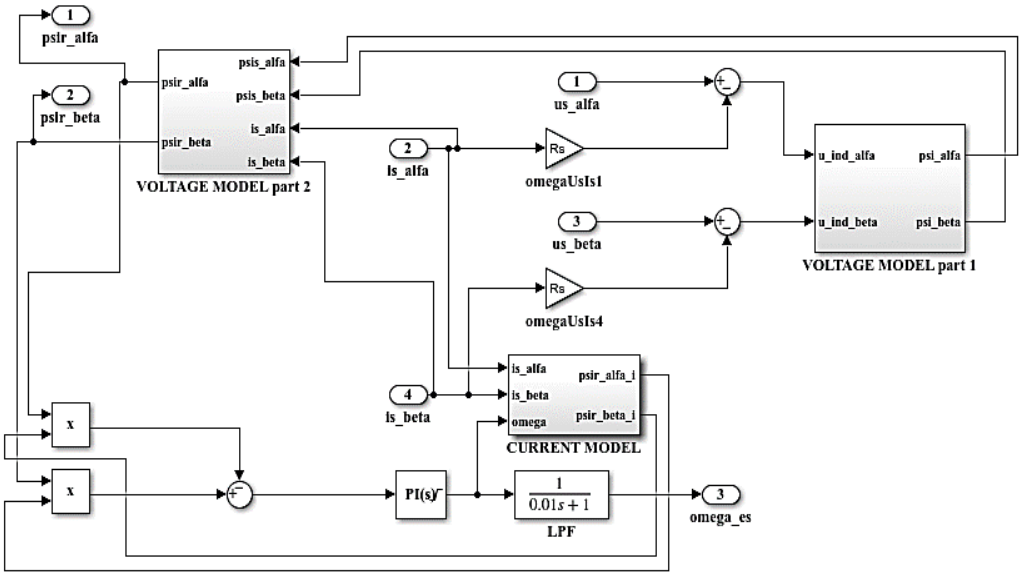

Figure 3: MRAS speed estimator in Simulink

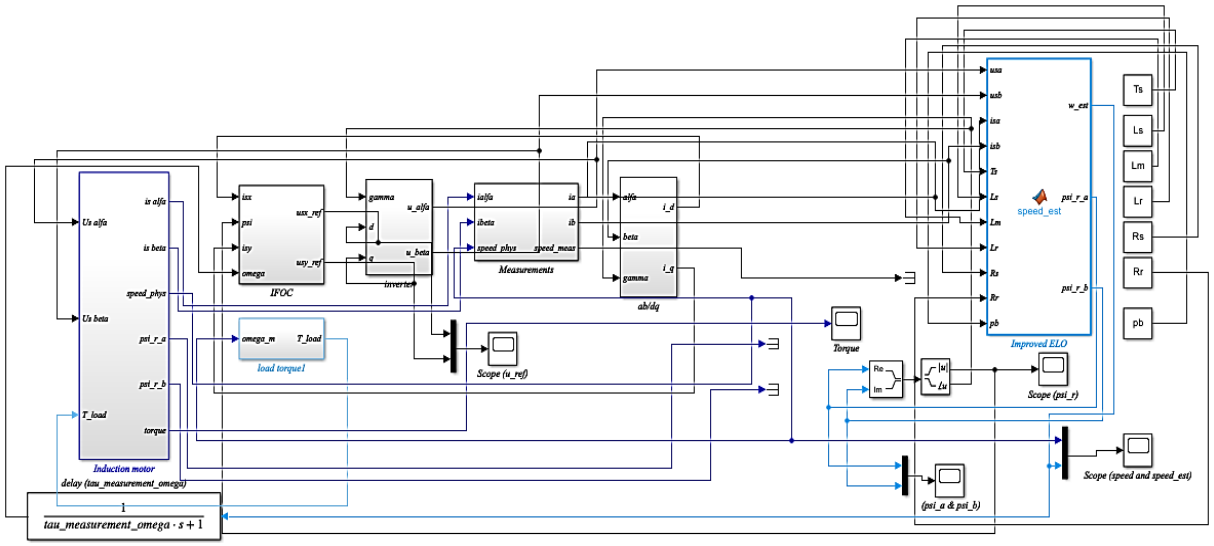

Figure 4: Overall ELO-based IM drive in Simulink

FOREX Publication
Open Access | Rapid and quality publishing
International Journal of Electrical and Electronics Research (IJEER)
Research Article | Volume 11, Issue 4 | Pages 1022-1029 | e-ISSN: 2347-470X

3. RESULT ANALYSIS

The Simulink model of MRAS speed estimator is shown in *figure 3*. Also, Sensorless IM drive model is implemented using MATLAB/Simulink software as shown in *figure 4*. Later, Simulation results are verified by using Snetly real-time controller. In this work, improved ELO and MRAS speed observer is implemented, and observed as follows:

Using ELO, the speed estimation of the induction motor is robust and has good speed tracking performance which is shown in *figure 5*. In this case, rotor reference speed is changed gradually from speed reversal to maximum speed of IM. Under various speed conditions, the motor speed is obtained very accurately without exceeding the speed estimation error. During t=1s to t=5s, the rotor speed under load is gradually increased from -100 rad/s to 150 rad/s. The motor is then tuned to maintain a constant speed of 150 rad/s between t=5 and t=6 seconds. The rotor reference speed is lowered from 150 rad/s to 125 rad/s between t=6 and t=7 seconds. At t= 8 s, the rotor reference speed is altered from 125 rad/s to -40 rad/s. Under loaded conditions, the motor is driven at t=8 s with rated torque and -100 rad/s, and then a step command of 100 rad/s is applied at t=8.2 s and removed at t=9.5 s. As a result, the drive's loading performance is good, and it maintains robust speed tracking performance under different circumstances, as shown above.

Also, the electromagnetic torque is developed as shown in *figure 6*. Also, *figure 7* and *figure 8* illustrate the reference flux and calculated rotor flux using ELO. The speed profile of the MRAS-based speed Sensorless IM drive is depicted in *figure 9*.

To comprehend and analyze the resilience of the drive under various timings in simulation, a step change in reference speed, ramp speed, and rapid change in reference speed are set in this. In this case, the anticipated speed serves as a feedback signal for the drive's closed-loop control. The speed prediction inaccuracy is really minimal, particularly in a steady condition, which is a good omen for the drive.

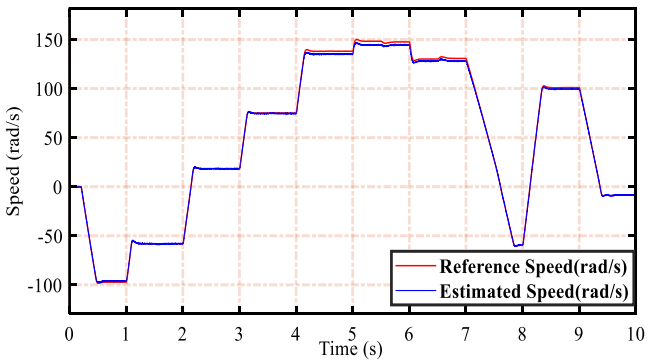

Figure 5: Speed profile using ELO-based IM drive

As explained speed profile in the ELO-based IM drive, MRAS speed-based drive is also subjected to load under different conditions to verify the robustness and its performance which is shown in *figure 10*.

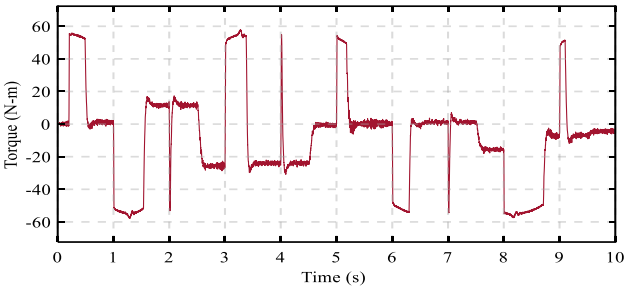

Figure 6: Electromagnetic torque in ELO-based IM drive

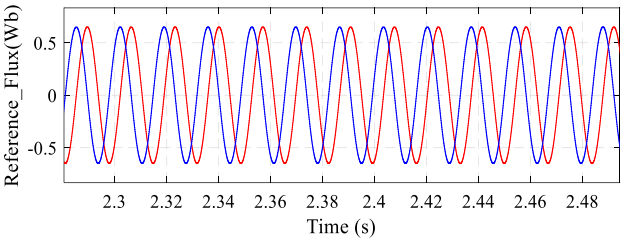

Figure 7: Reference flux generated in ELO-based IM drive

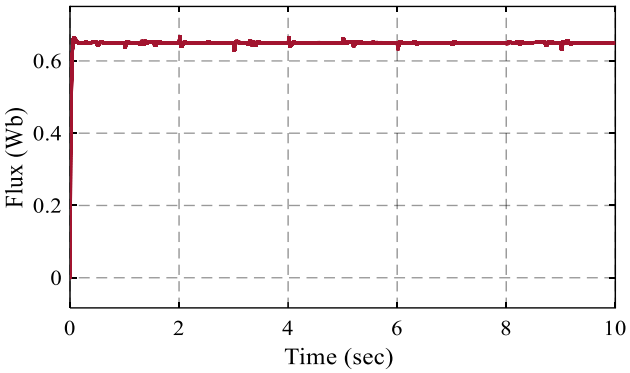

Figure 8: Estimation of rotor flux in ELO-based IM drive

Table 1: Induction Motor parameters

Squirrel Cage type 1.5 kW, 380 V, 14 A, 50 Hz, 4 poles, 1440 rpm		
Parameter	**Value**	**Units**
Stator Resistance, R_s	0.81	Ω
Rotor Resistance, R_r	0.49	Ω
Stator Inductance, L_s	264	mH
Rotor Inductance, L_r	372	mH
Magnetizing Inductance, L_m	0.1177	H

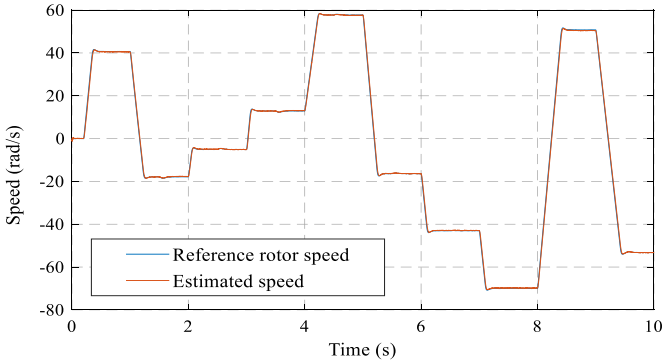

Figure 9: Speed profile of MRAS-based IM drive

FOREX Publication
Open Access | Rapid and quality publishing
International Journal of Electrical and Electronics Research (IJEER)
Research Article | Volume 11, Issue 4 | Pages 1022-1029 | e-ISSN: 2347-470X

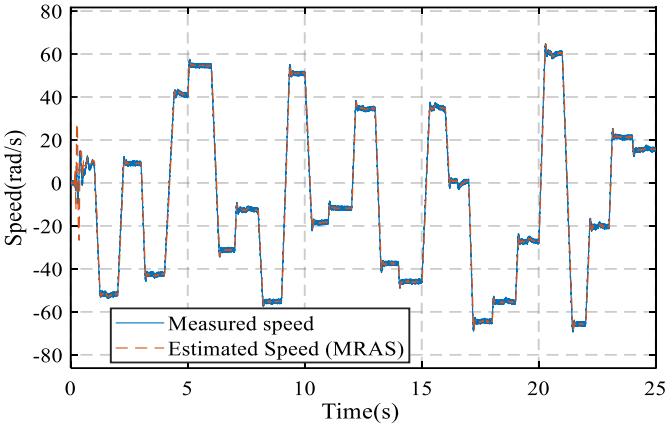

Figure 10: Speed profile of MRAS-based IM drive of different conditions

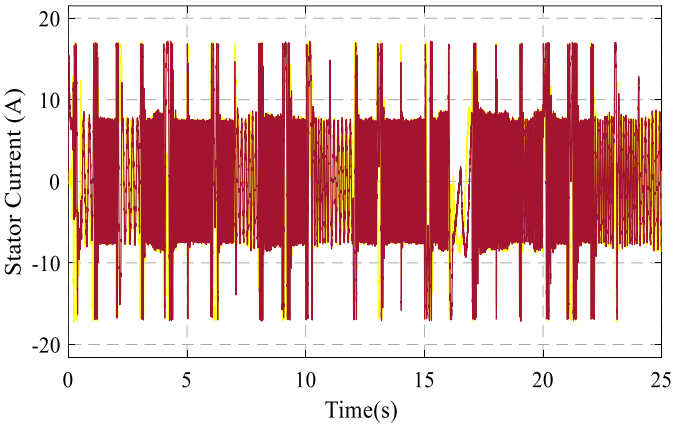

Figure 11: Stator current response in MRAS-based IM drive

At t=5 s, the rotor reference speed is set to 60 rad/s. Meanwhile, the motor is loaded with torque at t=4s and removed at t=15s, with a reference speed of 40 rad/s. A fast change in reference speed and speed reversal are also observed under load and no-load conditions. A difficulty with the IM drive's low-speed operation has been reported in the literature. The problem could have been corrected in this effort, resulting in good dynamic performance. The stator current response of the MRAS-based IM drive is shown in *figure 11*. The induction motor's parameters and values are shown in *table 1*.

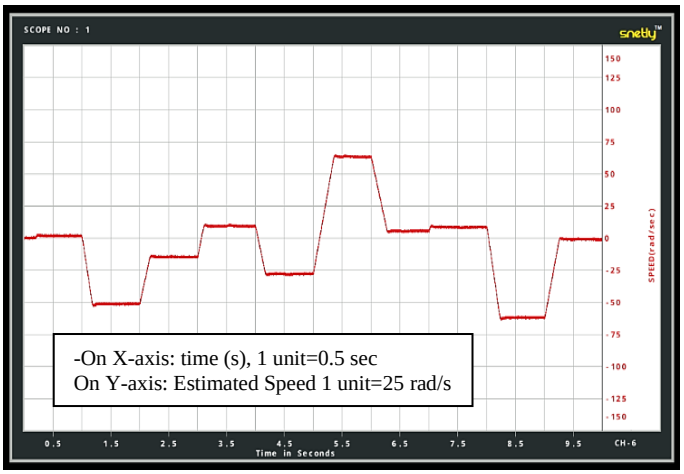

Figure 12: Speed profile of IM using ELO in Snetly

To verify the effectiveness and robustness of the improved techniques have been verified with the Snetly real-time controller. *Figure 12* shows the speed profile of an ELO control algorithm is tuned for IM drive whereas *figure 13* shows the speed profile of a MRAS-algorithm developed for IM drive. The performance comparison is shown between MRAS and ELO with conventional and improved algorithms as mentioned in *table 2*.

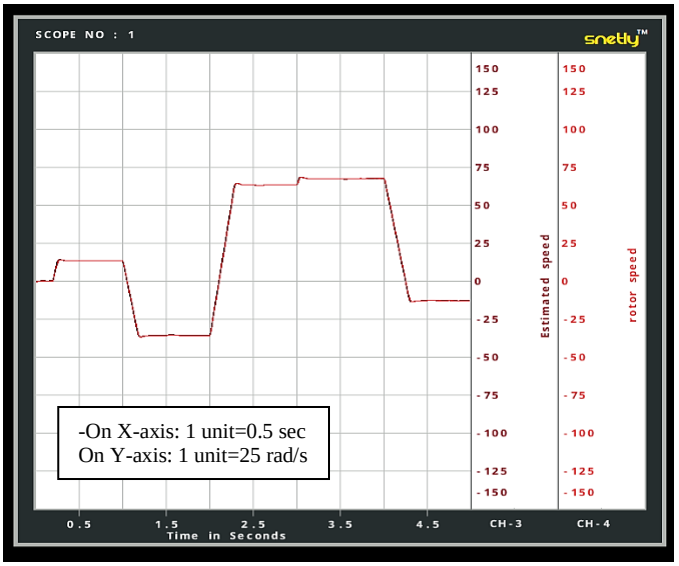

Figure 13: Speed profile of MRAS-based IM drive in Snetly

Table 2: Performance comparison: MRAS & ELO

Parameter	C-MRAS	Improved MRAS	C-ELO	Improved ELO
Speed Estimation	moderate	highest	medium	accurate
Speed Estimation error (%)	1.2	0.5	1.6	0.8
Speed tracking	medium	robust	low	medium
Stability	moderate	highest	low	medium
Speed profile (<10 rpm)	Medium	accurate	low	medium

Symbols and terms

$d-q$:rotating reference frame
ω_s:Synchronous speed
$(V_{sd}, V_{sq}), (I_{sd}, I_{sq})$: $d-q$ stator voltages and currents
$(\varphi_{rd}, \varphi_{rq})$: $d-q$ rotor fluxes
$\omega = p\,\Omega$:rotor speed
k:constant
$T_s = \frac{L_s}{R_s}$:stator time constant
$T_r = \frac{L_r}{R_r}$:rotor time constant
L_s, L_r:stator and rotor inductances
R_s, R_r:stator and rotor resistances
M:mutual inductance
p:number of pole pairs
C_e, C_r:electromagnetic and load torque
J:Total inertia

FOREX Publication
Open Access | Rapid and quality publishing
International Journal of Electrical and Electronics Research (IJEER)
Research Article | Volume 11, Issue 4 | Pages 1022-1029 | e-ISSN: 2347-470X

f_r:friction coefficient
E_d, E_q:compensation terms
φ_r:rotor flux
θ_s, θ:position of $d-q$ reference frame and the rotor
$\alpha-\beta$:stationary referenceframe
$(V_{s\alpha}, V_{s\beta}), (I_{s\alpha}, I_{s\beta})$: $\alpha-\beta$ stator voltages and currents
$(\varphi_{r\alpha})_{ref}, (\varphi_{r\beta})_{ref}$:the reference model$\alpha-\beta$ rotor fluxes
$(\varphi_{r\alpha})_{ad}, (\varphi_{r\beta})_{ad}$:the reference model$\alpha-\beta$ rotor fluxes
β:inverse of the rotor time constant
e_ω:error between reference and adjusted models
$\delta_\omega, \delta_{R_s}, \delta_\beta$:postive constants
K_p, K_i:controller adaptive gains
s:laplace operator
C-MRAS: conventional MRAS
C-ELO: conventional ELO

4. CONCLUSION

Speed Sensorless control algorithms are much popular in modern AC drives to behave similar to DC motor drives. The different topologies/improved methods have been suggested to achieve the performance of the drive. To address accurate speed estimation of actual speed with respect to the reference speed, reduced steady-state error i.e., difference between reference and actual speed and improved speed tracking (actual speed tracking to the reference speed), modern improved algorithms are required to be implemented in advanced real-time controllers. Also, such rapid prototype controllers are required for continuous monitoring of real-time control applications in power and industrial drives. In this work, improved ELO and MRAS observers have been implemented in MATLAB/Simulink software for speed Sensorless IM drive.

The results are quite satisfactory over different speed profile measurements and their estimations. The drive's performance has also been tested, and it is suited for low, medium, and high-speed applications. A Snetly real-time FPGA controller is also used to check and verify the Simulink findings. It is precise and suitable for in-the-moment observations. Robust speed tracking performance, lowered speed estimation error, and precise speed estimate are the main achievements noted and provided in this work. Future study on the stability and parameter sensitivity of various drives has the potential to build on this work.

Acknowledgments

The authors are thankful to AICTE- National doctoral fellowship (NDF/ADF) to enhance quality of research at Department of Electrical Engineering in Government College of Engineering (GCOE), Aurangabad, India.

REFERENCES

[1] M. Bermúdez, F. Barrero, C. Martín, and M. Perales, "Performance Analysis of Direct Torque Controllers in Five-Phase Electrical Drives," Appl. Sci., vol. 11, no. 24, p. 11964, Dec. 2021, doi: 10.3390/app112411964.

[2] R. Saifi, "Implementation of a new flux rotor based on model reference adaptive system for sensorless direct torque control modified for induction motor," Electr. Eng. Electromechanics, no. 2, pp. 37–42, Mar. 2023, doi: 10.20998/2074-272X.2023.2.06.

[3] K. Negadi, A. Mansouri, and R. Kourek, "Leonardo Electronic Journal of Practices and Technologies Hardware Implementation of Vector Control of Induction Motor Drive without Speed Encoder Using an Adaptive Luenberger Based MRAS Observer," Leonardo Electron. J. Pract. Technol., vol. 11, no. 20, pp. 99–114, 2012, [Online]. Available: http://lejpt.academicdirect.org.

[4] M. BabaLawan, A. Samaila, I. Tijjani, M. Mustapha, and M. A. Sarki, "Review of the Rotor Position and Speed Estimation Method of Induction Motor Drives." [Online]. Available: www.arcnjournals.org.

[5] M. S. Zaky, M. Khater, H. Yasin, and S. S. Shokralla, Review of Different Speed Estimation schemes for Sensorless Induction Motor Drives, no. JEE. 2018.

[6] A. G. M. A. Aziz, A. Y. Abdelaziz, Z. M. Ali, and A. A. Z. Diab, "A Comprehensive Examination of Vector-Controlled Induction Motor Drive Techniques," Energies, vol. 16, no. 6, p. 2854, Mar. 2023, doi: 10.3390/en16062854.

[7] S. Y. Maddu and N. R. Bhasme, "Performance analysis of Direct Torque Control of Induction Motor using Snetly real-time Controller," in 2022 19th International Conference on Electrical Engineering, Computing Science and Automatic Control (CCE), Nov. 2022, pp. 1–6, doi: 10.1109/CCE56709.2022.9975899.

[8] L. Et-Taaj, Z. Boulghasoul, A. Elkharki, Z. Kandoussi, and A. Elbacha, "Extended Kalman Filter for High performances Sensorless Induction Motor drive," Proc. 2019 IEEE World Conf. Complex Syst. WCCS 2019, 2019, doi: 10.1109/ICoCS.2019.8930736.

[9] M. Dal, "Enhancing sliding mode control with proportional feedback and feedforward: an experimental investigation on speed sensorless control of PM DC motor drives," doi: 10.3906/elk-1301-182.

[10] S. Y. Maddu and N. Ramesh Bhasme, "Performance Analysis of EKF-based Sensorless Induction Motor Drive using FPGA Controller," in 2023 13th International Symposium on Advanced Topics in Electrical Engineering (ATEE), Mar. 2023, pp. 1–6, doi: 10.1109/ATEE58038.2023.10108274.

[11] S. Yang et al., "A Novel Online Parameter Estimation Method for Indirect Field Oriented Induction Motor Drives," IEEE Trans. ENERGY Convers., vol. 32, no. 4, 2017, doi: 10.1109/TEC.2017.2699681.

[12] M. A. Fnaiech, J. Guzinski, M. Trabelsi, A. Kouzou, M. Benbouzid, and K. Luksza, "Mras-based switching linear feedback strategy for sensorless speed control of induction motor drives," Energies, vol. 14, no. 11, Jun. 2021, doi: 10.3390/en14113083.

[13] Y. Ren, R. Wang, S. J. Rind, P. Zeng, and L. Jiang, "Speed sensorless nonlinear adaptive control of induction motor using combined speed and perturbation observer," Control Eng. Pract., vol. 123, no. March, p. 105166, Jun. 2022, doi: 10.1016/j.conengprac.2022.105166.

[14] M. M. Almelian et al., "Enhancement of cascaded multi-level VSC statcom performance using ANN in the presence of faults," Int. J. Power Electron. Drive Syst., vol. 11, no. 2, pp. 895–906, 2020, doi: 10.11591/ijpeds.v11.i2.pp895-906.

[15] Z. Tir, T. Orlowska-Kowalska, H. Ahmed, and A. Houari, "Adaptive High Gain Observer Based MRAS for Sensorless Induction Motor Drives," IEEE Trans. Ind. Electron., pp. 1–9, 2023, doi: 10.1109/TIE.2023.3243271.

[16] Y. A. Zorgani, Y. Koubaa, and M. Boussak, "MRAS state estimator for speed sensorless ISFOC induction motor drives with Luenberger load torque estimation," ISA Trans., vol. 61, pp. 308–317, Mar. 2016, doi: 10.1016/j.isatra.2015.12.015.

[17] D. Bao, H. Wang, X. Wang, H. Wang, and C. Zhang, "Sensorless speed control based on the improved Q-MRAS Method for induction motor drives," Energies, vol. 11, no. 1, 2018, doi: 10.3390/en11010235.

[18] X. Han, Z. Li, M. Cabassud, B. Dahhou, and D. Boutaib, "A Comparison Study of Nonlinear State Observer Design: Application to an Intensified Heat-Exchanger," pp. 162–167, 2020, doi: 10.1109/MED48518.2020.9183148ï.

[19] Y. Li, H. Wu, X. Xu, X. Sun, and J. Zhao, "Rotor Position Estimation Approaches for Sensorless Control of Permanent Magnet Traction Motor in Electric Vehicles: A Review," World Electr. Veh. J., vol. 12, no. 1, p. 9, Jan. 2021, doi: 10.3390/wevj12010009.

International Journal of Electrical and Electronics Research (IJEER)
Research Article | Volume 11, Issue 4 | Pages 1022-1029 | e-ISSN: 2347-470X

[20] S. Mohan Krishna and J. L. Febin Daya, "MRAS speed estimator with fuzzy and PI stator resistance adaptation for sensorless induction motor drives using RT-lab," Perspect. Sci., vol. 8, pp. 121–126, Sep. 2016, doi: 10.1016/J.PISC.2016.04.013.

[21] M. Legesse, "'Speed Control of Vector Controlled PMSM Drive using Fuzzy Logic-PI Controller.'"

[22] X. Cheng, R. Song, G. Xie, Y. Zhang, and Z. Zhang, "A New FPGA-Based Segmented Delay-Line DPWM With Compensation for Critical Path Delays," IEEE Trans. Power Electron., vol. 33, no. 12, pp. 10794–10802, Dec. 2018, doi: 10.1109/TPEL.2017.2763750.

[23] Z. Chen, M. Yan, H. Fang, X. Zhang, D. Wu, and G. Luo, "Deadbeat Current Predictive Control for PMSM Drives Based on a Single FPGA with Digital Implementation Optimization," 2021, doi: 10.1109/PRECEDE51386.2021.9680970.

[24] Y. Luo, M. A. Awal, W. Yu, and I. Husain, "FPGA Implementation for Rapid Prototyping of High-Performance Voltage Source Inverters," CPSS Trans. POWER Electron. Appl., vol. 6, no. 4, pp. 320–331, 2021, doi: 10.24295/CPSSTPEA.2021.00030.

[25] J. Rivera Domínguez, I. Dueñas, and S. Ortega-Cisneros, "Discrete-Time Modeling and Control Based on Field Orientation for Induction Motors," IEEE Trans. POWER Electron., vol. 35, no. 8, pp. 8779–8793, 2020, doi: 10.1109/TPEL.2020.2965632.

[26] S. Bikash Santra, K. Bhattacharya, T. Roy Chudhury, and D. Chatterjee, "Generation of PWM Schemes for Power Electronic Converters," 2018.

[27] S. Y. Maddu and N. R. Bhasme, "Performance Investigation of Vector Control-based Induction Motor using Snetly Controller," Int. J. Electr. Electron. Eng., vol. 9, no. 12, pp. 109–119, Dec. 2022, doi: 10.14445/23488379/IJEEE-V9I12P109.

[28] K. K. Prabhakaran and A. Karthikeyan, "Electromagnetic Torque-Based Model Reference Adaptive System Speed Estimator for Sensorless Surface Mount Permanent Magnet Synchronous Motor Drive," IEEE Trans. Ind. Electron., vol. 67, no. 7, 2020, doi: 10.1109/TIE.2020.2965499.

[29] S. Krim, S. Gdaim, A. Mtibaa, and M. F. Mimouni, "Real time implementation of DTC based on sliding mode speed controller of an induction motor," in 2015 16th International Conference on Sciences and Techniques of Automatic Control and Computer Engineering (STA), Dec. 2015, pp. 94–100, doi: 10.1109/STA.2015.7505139.

[30] Z. Kandoussi, Z. Boulghasoul, A. Elbacha, and A. Tajer, "Sensorless control of induction motor drives using an improved MRAS observer," J. Electr. Eng. Technol., vol. 12, no. 4, pp. 1456–1470, 2017, doi: 10.5370/JEET.2017.12.4.1456.